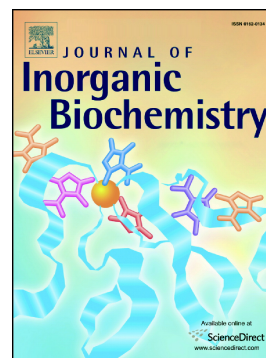


Journal Pre-proof

Detection of aluminum in lumbar spinal cord of sheep subcutaneously inoculated with aluminum-hydroxide containing products

Ricardo de Miguel, Javier Asín, Ana Rodríguez Largo, Jéssica Molín, Irache Echeverría, Damián de Andrés, Marta Pérez, Ignacio de Blas, Matthew Mold, Ramsés Reina, Lluís Luján



PII: S0162-0134(19)30515-X

DOI: <https://doi.org/10.1016/j.jinorgbio.2019.110871>

Reference: JIB 110871

To appear in: *Journal of Inorganic Biochemistry*

Received date: 30 July 2019

Revised date: 13 September 2019

Accepted date: 27 September 2019

Please cite this article as: R. de Miguel, J. Asín, A.R. Largo, et al., Detection of aluminum in lumbar spinal cord of sheep subcutaneously inoculated with aluminum-hydroxide containing products, *Journal of Inorganic Biochemistry* (2019), <https://doi.org/10.1016/j.jinorgbio.2019.110871>

This is a PDF file of an article that has undergone enhancements after acceptance, such as the addition of a cover page and metadata, and formatting for readability, but it is not yet the definitive version of record. This version will undergo additional copyediting, typesetting and review before it is published in its final form, but we are providing this version to give early visibility of the article. Please note that, during the production process, errors may be discovered which could affect the content, and all legal disclaimers that apply to the journal pertain.

Detection of Aluminum in Lumbar Spinal Cord of Sheep Subcutaneously Inoculated with Aluminum-Hydroxide Containing Products

#Ricardo de Miguel¹, #Javier Asín¹, Ana Rodríguez Largo¹, Jéssica Molín¹, Irache Echeverría², Damián de Andrés², Marta Pérez^{3,5}, Ignacio de Blas^{1,5}, Matthew Mold⁴, Ramsés Reina², *Lluís Luján^{1,5}

¹ Department of Animal Pathology, University of Zaragoza, Spain

² Institute of Agrobiotechnology, CSIC- Government of Navarra, Mutilva Baja, Navarra, Spain

³ Department of Animal Anatomy, Embryology and Genetics, University of Zaragoza, Spain

⁴ The Birchall Centre, Lennard-Jones Laboratories, Keele University, Staffordshire ST5 5BG, UK

⁵ Instituto Universitario de Investigación Mixto Agroalimentario de Aragón (IA2), University of Zaragoza, Spain

Both authors contributed equally

*Corresponding Author:

Lluís Luján

E-mail: Lluís.Lujan@unizar.es

Phone Number: (+34) 976 76 28 17

Postal Address: Miguel Servet street, 177.

Department of Animal Pathology.

University of Zaragoza.

C.P: 50017 (Zaragoza)

Spain

Abstract:

The use of vaccines containing aluminum (Al) adjuvants is widespread in ovine production. Al adjuvants induce an effective immune-response but lead to the formation of post-vaccination granulomas from which Al can disseminate. This work aims to study the accumulation of Al in the central nervous system of sheep subcutaneously inoculated with Al-hydroxide containing products. Lumbar spinal cord and parietal lobe from 21 animals inoculated with 19 doses of Vaccine (n=7), Adjuvant-only (n=7) or phosphate-buffered saline as Control (n=7) were analyzed with transversely heated graphite furnace atomic absorption spectroscopy and lumogallion staining for Al analytical measurements and Al tisular localization respectively. In the lumbar spinal cord, Al median content was higher in both the Adjuvant-only and Vaccine group (p=0.001) compared with the Control group. Animals of the Adjuvant-only group showed the higher individual measurements in the lumbar spinal cord (14.36 µg/g and 7.83 µg/g). In the parietal lobe, Al median content tended to be higher in the Adjuvant-only group compared with Control group (p=0.074). Except for three replicates of the Adjuvant-only group, Al content was always below 1 µg/g. In the lumbar spinal cord, lumogallion reactive Al deposits were more abundant in the gray matter than in the white matter in both Vaccine (p=0.034) and Adjuvant-only groups (p=0.017) and Al deposits were mostly associated with glial-like cells (p= 0.042). In the parietal lobe, few Al deposits, which were sometimes related to vessels, were found. In sheep, Al-hydroxide adjuvants inoculated in the subcutaneous tissue selectively accumulates in the lumbar spinal cord.

Keywords: Aluminum hydroxide; Aluminum-based vaccines; sheep; ovine; central nervous system

1. Introduction

Vaccines are key elements for controlling diseases in animal populations. From the 1930s, vaccines have made a major contribution to improving sheep health, welfare and productivity [1]. The ovine health programs in South-Europe usually involve vaccination against common reproductive, digestive and respiratory pathogens [2]. The vaccination schedule of each flock largely depends on management system, production type, breed and local climate [2]. In our local conditions (meat-producing breeds managed in semi-intensive to intensive systems that often implies shepherding), animals usually receive between 2-4 vaccines per year during their whole lifespan.

The majority of modern vaccines need an adjuvant to strengthen the humoral and cellular immune responses induced against the vaccine antigen [3]. Most ovine vaccines use aluminum (Al) hydroxide as adjuvant which induces a fast and effective immune-response against vaccine antigens. This adjuvant consists of primary nano-sized particles that spontaneously aggregate forming micron-sized agglomerates subjected to marked size variations depending on Al-hydroxide concentration, ionic strength of the diluent and antigen absorption [4,5]. The mechanism of action of Al-hydroxide adjuvants remains unclear although recent data indicate that stimulation of the inflammasome may play a major role [6,7].

A variety of post-vaccination secondary effects have been described in animal species [8–12]. Specifically, in sheep, Al-based vaccines have been associated with the ovine autoimmune/inflammatory syndrome induced by adjuvants (ovine ASIA syndrome) [13]. This complex syndrome was described after the compulsory European vaccination campaigns against bluetongue virus of ruminants and can still be detected nowadays associated with other vaccines that contain Al-hydroxide as adjuvant [14].

In sheep, Al-hydroxide is phagocytosed by macrophages inducing the formation of persistent sterile subcutaneous granulomas, from which intracytoplasmic Al-hydroxide can translocate by leukocyte trafficking to the regional lymph node [15]. In mice, lymph node plays a key role in Al biodistribution enabling intramacrophagic Al to reach distant tissues such as the spleen and central nervous system (CNS) [16,17]. Whether Al-hydroxide can reach other locations in the sheep body after subcutaneous injection of Al-hydroxide alone or formulated in Al-based vaccines is unknown. The aim of this work is to determine the presence of Al in the CNS of sheep after subcutaneous injection of Al-hydroxide containing products and to study the localization of this Al within the neuroparenchyma.

2. Materials and Methods

2.1. Animals

All experimental procedures were approved and licensed by the Ethical Committee of the University of Zaragoza (PI15/14). Animal samples analyzed in this work belonged to a previous, wider study carried out by our group that aimed to study the local and systemic effects caused by repetitive subcutaneous inoculation of Al-containing adjuvants in sheep [15]. Briefly, twenty-one, three-month-old, neutered male purebred Rasa Aragonesa lambs were selected from a pedigree flock of certified good health and lodged indoor at the experimental farm of the University of Zaragoza, with optimal conditions of housing, management and diet for 15 months.

Based on the received treatment, animals were divided into 3 groups of 7 animals each and were inoculated with different substances: Vaccine group was treated with commercial vaccines, Adjuvant-only group was inoculated with Al-hydroxide (Alhydrogel ®, CZ Veterinaria, Spain) and Control group

received phosphate-buffered saline (PBS). Animals had never been vaccinated or inoculated with any other substance prior to the experiment. Lambs underwent an accelerated vaccination scheduled to mimic, in an acceptable time frame for an experimental project, the AI load that these animals can receive in field conditions during their lifespan. Inoculations were performed in the subcutaneous tissue of the flank. A total of 19 inoculations were distributed in 15 injection dates. The schedule of injections for the three groups and the vaccines used are detailed in Figure S1 and Table S1 respectively. AI content of each inocula was measured by inductively coupled plasma mass spectrometry. Vaccine and Adjuvant-only groups received a total of 81,29 mg of AI per animal. AI content of PBS inocula was always under the limit of detection of the technique (0.074 µg/mL). At the end of the study animals were euthanished and systematic tissue sampling was performed.

2.1. Aluminum content in lumbar spinal cord and parietal lobe

AI content in the lumbar spinal cord and the parietal cerebral lobe was determined in all animals by transversely heated graphite atomic absorption spectroscopy (TH-GFAAS) using an established method [18]. Briefly, three replicate portions of 0.3-0.5 g from the parietal lobe and lumbar spinal cord of each animal were dried in a 37°C incubator until reaching a constant weight. A mixture of 1 mL 15.8 M HNO₃ and 1 mL of 30 % w/v H₂O₂ was used to digest each replicate in a microwave (MARS Xpress CEM Microwave Technology Ltd.). After digestion, samples were diluted with ultrapure water to reach a final volume of 5 mL. Total AI content was measured by an atomic absorption spectrometer with a transversely heated graphite atomizer and longitudinal Zeeman-effect background corrector and an AS-80 autosampler with WinLab32 software (Perkin Elmer, UK). Determinations were calculated by using the Zeeman background corrected peak area of the atomic absorption

signal and each determination was the arithmetic mean of three sample injections with a relative standard deviation of 10 %. Results were expressed as $\mu\text{g Al/g}$ tissue dry weight.

2.2. Aluminum localization in lumbar spinal cord and parietal lobe

Lumogallion staining was performed in formalin-fixed paraffin-embedded tissues of the lumbar spinal cord and parietal lobe following a recently validated method which is highly specific for Al detection in tissues [19]. Briefly, 5 μm -thick tissue sections carefully protected from environmental Al contamination were dewaxed, rehydrated and incubated for 45 minutes with a 1 mM solution of lumogallion (Tokyo Chemical Industry, UK) buffered in 50 mM 1,4-Piperazine-diethanesulfonic acid buffer (PIPES-buffer) pH 7.4. Serial sections from each tissue were used as controls for evaluation of tissue autofluorescence. The control sections followed the same protocol but they were incubated only with PIPES-buffer solution. After incubation, all slides were washed 6 times with PIPES-buffer solution, rinsed in ultrapure water, mounted with an aqueous medium and stored at 4°C overnight prior to analysis. Lumogallion and control autofluorescence analyses were performed using a fluorescence microscope (Zeiss AxioVert 200M, Germany) with a bandpass excitation filter (470/40 nm), beam splitter (495nm) and bandpass emission filter (590/33 nm). Excitation of the Al-lumogallion complex emits characteristic yellow-orange fluorescence. Autofluorescence of immediately adjacent serial sections confirmed lumogallion fluorescence as indicative of Al staining. Images were taken with AxioCam HR and processed with analyses software package AxioVision 4.6.3. Total evaluated area was approximately 200 mm^2 in the parietal lobe and approximately 50 mm^2 in the lumbar spinal cord.

2.2. Statistical analysis

Shapiro-Wilk's test was used to check if the data of the quantitative variables (i.e. Al content and Al deposits) met the assumptions of normality. As none of them met the assumptions, they were considered non-normal, thus they were described using median and interquartile range (IQR). Data were graphically represented using box and whiskers plots, where boxes represent the IQR ($IQR=Q3-Q1$) and contain 50 % of the data. Whisker bars were calculated from the IQR (Upper: $Q3 + 1.5 \times IQR$; lower: $Q1 - 1.5 \times IQR$), and reflect the variability of the data outside Q1 and Q3.

In non-normal non-paired variables (i.e. comparisons of the content in Al in the CNS among the three groups) association of a non-normal quantitative variable with a qualitative variable with three or more categories was assessed by Kruskal-Wallis test followed by post hoc Dunn's test [20]. In non-normal paired variables (i.e. comparisons of Al deposits in the gray matter and white matter) the association between variables was assessed by Wilcoxon test [20].

3. Results

3.1. Aluminum content in lumbar spinal cord and parietal lobe

The content of Al within all tissue replicates measured in the lumbar spinal cord is detailed in Table 1. Only in the Control group were more than half of the replicates (11/21, 52 %) below 0.01 $\mu\text{g/g}$. Two animals (111 and 113) within the Adjuvant-only group presented two high (over 2 $\mu\text{g/g}$) replicates each. Adjuvant-only and Vaccine groups (Adjuvant-only: median=0.49 $\mu\text{g/g}$, IQR=0.31-1.04; Vaccine: median=0.39 $\mu\text{g/g}$, IQR=0.33-0.62) showed a significantly ($p=0.001$) higher Al content than the Control group (median=0.08 $\mu\text{g/g}$, IQR=0.01-0.44). A comparison between groups is shown in Figure 1.

The content of Al within all tissue replicates measured in the parietal lobe is detailed in Table 2. Replicates in the three groups were homogeneous, with most of the values below 1 µg/g. Within the Adjuvant-only group there were three replicates over this value. Al content in the Adjuvant-only group (median=0.2 µg/g, IQR=0.11-0.73) tended to be higher ($p=0.074$) when compared with the Control group (median=0.1 µg/g, IQR=0.01-0.26) whereas none of these two groups differed with the Vaccine group (median=0.1 µg/g, IQR=0.01-0.35). A comparison between groups is shown in Figure 2.

3.2. Aluminum localization in lumbar spinal cord and parietal lobe

Details of Al deposits found in the CNS (lumbar spinal cord and parietal lobe) are shown in Tables S2 and S3. Lumogallion reactive deposits, showing a yellow-orange fluorescence emission were observed in both, lumbar spinal cord and parietal lobe and they were identified as Al after autofluorescence verification. The vast majority of Al deposits were located in the gray matter, they were micron-sized (1-10µm approx.) and were mostly cell-associated. Deposits were significantly more abundant in the lumbar spinal cord than in the parietal lobe in the Adjuvant-only group ($p=0.027$) and they showed a marked trend in the Vaccine group ($p=0.054$). All animals of the Adjuvant-only group and Vaccine group showed at least one Al deposit in the lumbar spinal cord. The total number of deposits at lumbar spinal cord were similar in Vaccine (22) and Adjuvant-only (21) groups and they significantly differed ($p=0.002$ and $p=0.001$ respectively) from the Control group (2). In the lumbar spinal cord, Al deposits were significantly more abundant in the gray matter (Figure 3) than in the white matter in both Vaccine ($p= 0.034$) and Adjuvant-only ($p= 0.017$) groups. Al deposits in the gray matter of the lumbar spinal cord were observed mostly associated with morphologically compatible glial cells

(Figure 4a, 4b) and only a few deposits were non-cell associated (Figure 4c, 4d), this difference being statistically significant ($p= 0.042$).

In the parietal lobe, Al was mostly found in the gray matter of the Vaccine group, in sharp contrast to Adjuvant-only ($p=0.017$) and Control groups ($p=0.017$). These deposits were cell-associated and sometimes closely related to vessels (Figure 5). The Al deposits observed in the parietal lobe was strikingly lower in contrast with the deposits found in the lumbar spinal cord (Tables S2 and S3).

4. Discussion

In sheep, Al-containing products lead to the formation of subcutaneous granulomas from where intramacrophagic Al-hydroxide can reach the regional lymph node and potentially disseminate to other organs [15]. This is the first work that studies accumulation of Al in the CNS of sheep after subcutaneous, repeated injections of Al-containing products. Al was quantitatively measured by TH-GFAAS and localized by lumogallion staining in lumbar spinal cord and parietal lobe.

The Adjuvant-only and Vaccine groups presented higher Al levels in the spinal cord compared with the Control group. The difference was more marked in the Adjuvant-only group and, indeed, the highest individual replicates were obtained in animals from this group. One animal in the Adjuvant-only group presented two replicates of 2.14 $\mu\text{g/g}$ and 14.36 $\mu\text{g/g}$ each, while another presented two replicates of 7.83 $\mu\text{g/g}$ each. The variability between replicates within the same animal is attributed to the characteristic patchy distribution of Al within tissues, which does not diffuse homogeneously [18,19,21]. In measurements performed in human brain tissue with this technique, replicate values over 2 $\mu\text{g/g}$ were considered high and potentially

pathologic [19]. The Vaccine group did not show high replicates in the lumbar spinal cord. The highest measurement in this group was 1.23 µg/g. Nevertheless, the median Al levels were significantly higher than in the Control group, which showed similar low levels to the brain tissue. Interestingly, more than half (11/21, 52%) of all replicates measured in the lumbar spinal cord of the Control group were below 0.1 µg/g.

The presence of higher lumbar spinal cord levels of Al in the Adjuvant-only group than in the Vaccine group could be related to the demonstrated decreased persistence of post-vaccination granulomas at the subcutaneous level in the Adjuvant-only group and also to the smaller size of Al particles contained in intramacrophagic aggregates [15]. It is known that size of Al-hydroxide aggregates depends on Al-hydroxide concentration, ionic strength of the milieu and antigen affinity [5]. Shardlow *et al.* have shown that prior to the inoculation into the animal, Al-hydroxide aggregates present in the inocula are notably larger in vaccine formulations (4,2 µm median size) in contrast with Adjuvant-only solutions diluted into physiological saline (2,8 µm median size) [5]. The optimal size range of particles for macrophagic phagocytosis is 2-3 µm [22]. In vitro studies show that larger size of Al-hydroxide aggregates is related with delayed macrophagic internalization and increased cell toxicity and death [6,23]. This scenario could explain the earlier mobilization and systemic distribution of Al from the granulomas in the Adjuvant-only group as well as the increased cell death and necrosis observed in the Vaccine group [15]. Actually, murine studies show that the size of Al-adjuvant particles play a key role in systemic Al biodistribution and their accumulation in the CNS [16,17]. Interestingly, in mice this accumulation is inversely related to the persistence of the intramuscular post-vaccination granuloma [17].

Most of the replicates measured in the parietal lobe were within the same limits in the three treatment groups. Just the Adjuvant-only group presented a few slightly higher replicates. This is similar to some findings observed in mice inoculated intramuscularly, which failed to demonstrate AI accumulation in the brain at 270 days after first inoculation, although subcutaneous inoculation in a subsequent experiment demonstrated translocation of AI adjuvants into the CNS [24]. In our large animal experimental model, maybe the 15-month experiment was not long enough to permit significant AI input into the CNS.

As our data represents the first AI measurements performed in ovine nervous tissue (Tables 1 and 2) the values obtained in the Control group will be considered as the reference values for normal AI levels in sheep: this being so, a range of 0.01 – 0.26 µg/g with a median of 0.1 µg/g in the brain; and a range 0.01 – 0.44 µg/g with a median of 0.08 µg/g in the lumbar spinal cord. These values contribute to the set of levels established in other models, such as mice, rats, and rabbits [25–28], and will be the starting point for further studies to be performed in sheep.

Lumogallion is a highly specific fluorescent stain for AI localization in CNS [19] that has been widely validated in a variety of animal species [15,29,30] and is useful for detecting AI adjuvants [31,32]. In this study, AI was primarily located in the gray matter and was usually associated with glial-like cells in sections from both, lumbar spinal cord and parietal lobe. In agreement with the analytical measurements of AI obtained by TH-GFAAS, lumogallion reactive AI deposits were more abundant in the lumbar spinal cord than in the parietal lobe. The former location showed more AI deposits than the latter, what is in concordance with the results obtained by TH-GFAAS. Interestingly, in the parietal lobe AI was found in close proximity to blood vessels and it was likely intracellular (Fig. 5). Despite the scarce number of deposits found at this

location, the presence of this vascular-associated Al particles could support the hypothesis of the hematogenous dissemination of Al-loaded macrophages from the regional lymph node via the efferent lymphatics and the thoracic duct [16]. In the lumbar spinal cord, most Al deposits were found likely associated with glial cells, something that has been previously described in translocation studies of intramuscularly inoculated Al based adjuvants in mice [16,17]. The prevalence of Al-associated glial-like cells reinforce the idea of an Al input to the CNS via Al-loaded macrophages [16]. Indeed, previous studies in mice have demonstrated Al particles within astroglial and microglial cells [16]. Moreover, Al-hydroxide has been shown to increase microglial cell density in mice [17].

All lumogallion positive deposits found in the present study were dense micron-sized aggregates of Al that were predominantly cell-associated and located in the gray matter. Such characteristics were similar to those described in murine studies of Al adjuvants distribution [16]. However, these results contrast with other studies in which Al of unknown origin and composition was also found in human CNS as diffuse and plaque-like deposits [30,33]. Our results may suggest that both different routes of entry and different chemical compositions of Al components, may play a major role in the distribution and histopathological morphology of Al in the CNS.

A limitation of the study could be the number of CNS samples analyzed. The three replicates used to quantitatively determine Al levels represented a total of 0.9–1.5 g per brain, which accounts for about 1% of the total brain weight [34]. Likewise, Al detection in tissue sections by fluorescence microscopy also represented a limited sampling of the CNS. Another limitation of the study could be the accelerated vaccination schedule. Although the recommended protocols for each individual product were always fulfilled, this

experimental vaccination schedule was designed to be able to detect clinicopathologic changes in experimental animals within 15 months. The outcome of the same amount of AI divided in small doses for a longer period of time might differ from the results of the present study.

In any case, our results suggest that sheep selectively accumulate subcutaneously injected AI in the lumbar spinal cord. This selective accumulation of AI may be due to morphological and physiological differences between the blood-brain barrier (BBB) and the blood-spinal cord barrier (BSCB) [35]. In normal conditions, BSCB present decreased expression of tight junction proteins (ZO-1 and occludin) and adherence junction proteins (VE-cadherin and β -catenin) and it is more permeable to proinflammatory cytokines as IFN γ and TNF α than BBB [35,36]. Moreover, studies in mice shows that IFN γ passage through the BBB is saturated at low doses whereas BSCB remains non saturated in the lumbosacral region at the same doses [36]. This increased permeability in the lumbar spinal cord has been proposed to play a role in certain processes such as experimental immune encephalomyelitis [37]. This permeability could also account for different input of AI into the CNS either by a direct mechanism, favoring the leukocyte trafficking or indirectly, accelerating a local neuroinflammatory status which has already been related with higher AI input into the CNS [16,37]. Alternatively, a weak BSCB at the lumbar area may be contributing to this selective accumulation as already demonstrated in mice with a leaky BBB [16].

Selective accumulation of AI in the lumbar spinal cord could be linked to the lesions observed in the chronic phase of the ovine ASIA syndrome, where neurodegenerative changes were mostly observed at the lumbar spinal cord [13]. Moreover, these AI deposits might contribute to the development of

neuropathological problems as Al is a potential neurotoxic molecule [38]. In this sense, animals of the Vaccine and Adjuvant-only groups exhibited behavioral changes, characterized by decreased affiliations, increased aggressive interactions, and increased stereotypies together with increased cortisol levels (J. Asín, manuscript in preparation). Complete histopathological study of the CNS is currently being performed to further clarify these aspects.

5. Conclusions

Al analytical measurements and fluorescent Al deposits indicate that, in sheep, the subcutaneous and intensive injection of Al adjuvants increase the levels of Al in the lumbar spinal cord.

6. Table of Abbreviations

Al:	Aluminum
ASIA:	Autoimmune/Inflammatory Syndrome Induced by Adjuvants
CNS:	Central Nervous system
PBS:	Phosphate-buffered saline
TH-GFAAS:	Transversely Heated Graphite Atomic Absorption Spectroscopy
PIPES-buffer:	1,4-Piperazine-diethanesulfonic acid buffer
IQR:	Interquartile Range
BBB:	Blood-brain barrier
BSCB:	Blood-spinal cord barrier

6. Acknowledgments: We deeply thank Victor Sorribas for his kind help with the fluorescence studies. Charo Puyó and Santiago Becerra are acknowledged for their technical support.

7. Funding: RM is a PhD student funded by the Department of Innovation, Research and University of Aragon, Spain. JA and ARL are PhD students funded by the Spanish Ministry of Science, Innovation and Universities (formerly Spanish Ministry of Education). This work was funded by grants from the Spanish Ministry of Economy and Industry (AGL2013-49137-C3-1-R and RTI2018-096172-B-C33), the Ministry of Science, Innovation and Universities (RTI2018-096172-B-C31 and RTI2018-096172-B-C33) and the Government of Aragón (A17_17R, Animal Health and Reproduction).

8. Author Contributions: RM and JA equally contributed to this work and wrote the manuscript. RM, ARL, IE and MM performed and interpreted the lumogallion studies. JA performed and interpreted the TH-GFAAS studies. RM, JA, JM and NB performed the statistical and critical analysis of the data obtained. DA, RR, MP and LL were in charge of conceptualization of the work, methodology followed, funding acquisition and project administration.

Conflicts of Interest: Authors declare no conflicts of interest with respect to the research, authorship and/or publication of this article.

9. References

- [1] Guidelines: Responsible use of vaccines and vaccination in sheep production, in RUMA Alliance, 2009, pp. 1-29.
- [2] D. Lacasta, L.M. Ferrer, J.J. Ramos, J.M. González, A. Ortín, G.C. Fthenakis, *Vet. Microbiol.* 181 (2015) 34–46.
- [3] T.B. Ruwona, H. Xu, X. Li, A.N. Taylor, Y.-C. Shi, Z. Cui, *Vaccine*. 34 (2016) 3059–3067.
- [4] H. Eidi, M.O. David, G. Crépeaux, L. Henry, V. Joshi, M.H. Berger, M. Sennour, J. Cadusseau, R.K. Gherardi, P.A. Curmi, *BMC Med.* 13 (2015) 114
- [5] E. Shardlow, M. Mold, C. Exley, *Front. Chem.* 4 (2016) 48.
- [6] E. Shardlow, M. Mold, C. Exley, *Allergy Asthma Clin. Immunol.* 14 (2018) 80.
- [7] S.C. Eisenbarth, O.R. Colegio, W. O'connor, F.S. Sutterwala, R.A. Flavell, *Nature*. 453 (2008) 1122–1126.
- [8] K. Ohmori, K. Masuda, M. Sakaguchi, Y. Kaburagi, K. Ohno, H. Tsujimoto, *J. Vet. Med. Sci.* 64 (2002) 851–853.
- [9] G.E. Moore, N.W. Glickman, M.P. Ward, K.S. Engler, H.B. Lewis, L.T. Glickman, *J. Am. Vet. Med. Assoc.* 226 (2005) 909–912.
- [10] G.E. Moore, L.F. Guptill, M.P. Ward, N.W. Glickman, K.K. Faunt, H.B. Lewis, L.T. Glickman, *J. Am. Vet. Med. Assoc.* 227 (2005) 1102–1108.
- [11] T. Tung, D. Phalen, J. A. Toribio, *Aust. Vet. J.* 93 (2015) 405–411.
- [12] J.L. Valli, *Can. Vet. J.* 56 (2015) 1090–1092.
- [13] L. Luján, M. Pérez, E. Salazar, N. Álvarez, M. Gimeno, P. Pinczowski,

- S. Irusta, J. Santamaría, N. Insausti, Y. Cortés, L. Figueras, I. Cuartielles, M. Vila, E. Fantova, J.L.G. Chapullé, *Immunol. Res.* 56 (2013) 317–324.
- [14] J. Asín, M. Pérez, P. Pinczowski, M. Gimeno, L. Luján, *Immunol. Res.* 66 (2018) 777–782.
- [15] J. Asín, J. Molín, M. Pérez, P. Pinczowski, M. Gimeno, N. Navascués, A. Muniesa, I. de Blas, D. Lacasta, A. Fernández, L. de Pablo, M. Mold, C. Exley, D. de Andrés, R. Reina, L. Luján, *Vet. Pathol.* 56 (2019) 418–428.
- [16] Z. Khan, C. Combadière, F.-J. Authier, V. Itier, F. Lux, C. Exley, M. Mahrouf-Yorgov, X. Decrouy, P. Moretto, O. Tillement, R.K. Gherardi, J. Cadusseau, *BMC Med.* 11 (2013).
- [17] G. Crépeaux, H. Eidi, M.O. David, Y. Baba-Amer, E. Tzavara, B. Giros, F.J. Authier, C. Exley, C.A. Shaw, J. Cadusseau, R.K. Gherardi, *Toxicology.* 375 (2017) 48–57.
- [18] E. House, M. Esiri, G. Forster, P.G. Ince, C. Exley, *Metallomics.* 4 (2012) 56–65.
- [19] A. Mirza, A. King, C. Troakes, C. Exley, *J. Alzheimer's Dis.* 54 (2016) 1333–1338.
- [20] W.W. Daniel, C.L. Cross, *Biostatistics: a foundation for analysis in the health sciences*, John Wiley & Sons Inc., Singapore, 2013.
- [21] D.R.C. McLachlan, C. Bergeron, P.N. Alexandrov, W.J. Walsh, A.I. Pogue, M.E. Percy, T.P.A. Kruck, Z. Fang, N.M. Sharfman, V. Jaber, Y. Zhao, W. Li, W.J. Lukiw, *Mol. Neurobiol.* 56 (2019) 1531–1538.
- [22] J.A. Champion, A. Walker, S. Mitragotri, *Pharm. Res.* 25 (2008) 1815.

- [23] M. Mold, E. Shardlow, C. Exley, *Sci. Rep.* 6 (2016) 31578.
- [24] G. Crépeaux, H. Eidi, M.O. David, E. Tzavara, B. Giros, C. Exley, P.A. Curmi, C.A. Shaw, R.K. Gherardi, J. Cadusseau, *J. Inorg. Biochem.* 152 (2015) 199–205.
- [25] P.I. Oteiza, C.L. Keen, B. Han, M.S. Golub, *Metabolism.* 42 (1993) 1296–300.
- [26] K. Demirkaya, B.C. Demirdöğen, Z.Ö. Torun, O. Erdem, E. Çırak, Y.M. Tunca, *Hum. Exp. Toxicol.* 36 (2017) 1071–1080.
- [27] H.B. Röllin, P. Theodorou, T.A. Kilroe-Smith, *Br. J. Ind. Med.* 48 (1991) 389–391.
- [28] G. Sahin, I. Varol, A. Temizer, K. Benli, R. Demirdamar, S. Duru, *Biol. Trace Elem. Res.* 41 (1994) 129–135.
- [29] C.S. Martinez, A.G. Escobar, J.A. Uranga-Ocio, F.M. Peçanha, D.V. Vassallo, C. Exley, M. Miguel, G.A. Wiggers, *Reprod. Toxicol.* 73 (2017) 128–141.
- [30] M. Mold, J. Cottle, C. Exley, *Int. J. Environ. Res. Public Health.* 16 (2019) 2129.
- [31] M. Mold, H. Eriksson, P. Siesjö, A. Darabi, E. Shardlow, C. Exley, *Sci. Rep.* 4 (2014).
- [32] I. Mile, A. Svensson, A. Darabi, M. Mold, P. Siesjö, H. Eriksson, *J. Immunol. Methods.* 422 (2015) 87–94.
- [33] M. Mold, A. Chmielecka, M. Rodriguez, F. Thom, C. Linhart, A. King, C. Exley, *Int. J. Environ. Res. Public Health.* 15 (2018) 1777.
- [34] S. Louey, M.L. Cock, R. Harding, *J. Reprod. Dev.* 51 (2005) 59–68.

- [35] V. Bartanusz, D. Jezova, B. Alajajian, M. Digicaylioglu, *Ann. Neurol.* 70 (2011) 194–206.
- [36] W. Pan, W.A. Banks, A.J. Kastin, *J. Neuroimmunol.* 76 (1997) 105–111.
- [37] P.M. Daniel, D.K.C. Lam, O.E. Pratt, *J. Neurol. Sci.* 52 (1981) 211–219.
- [38] S. Maya, T. Prakash, K. Das Madhu, D. Goli, *Biomed. Pharmacother.* 83 (2016) 746–754.

Journal Pre-proof

10. Figure captions

Figure 1. Aluminum (Al) content in the lumbar spinal cord in sheep of the Control group, Adjuvant-only group and Vaccine group.

Figure 2. Aluminum (Al) content in the parietal lobe in sheep of the Control group, Adjuvant-only group and Vaccine group.

Figure 3. Sheep 111, Adjuvant-only group, gray matter of the lumbar spinal cord. (a-b) Lumogallion staining. Two intense yellow-orange fluorescent aluminum (Al) deposits (asterisk and arrow head) depicting the fluorescence channel (a) and bright field overlay (b). (c-d) Sequential unstained sections for autofluorescence evaluation (asterisk and arrow head indicates the same area as Al deposits were found with lumogallion). A green autofluorescence emission background was identified in non-stained sections, confirming the specific staining of Al deposits found in (a) and (b), respectively. Note weakly autofluorescent intraneuronal pigments of lipofuscin (arrow) shown in both the lumogallion stained (a) and the non-stained sections (c) under fluorescent channel. Scale bar: 20 μ m.

Figure 4. Sheep 111, Adjuvant-only group, gray matter of the lumbar spinal cord. Higher magnification of deposits seen in Figure 3. Lumogallion staining. Two intense yellow-orange fluorescent aluminum (Al) deposits (asterisk and arrowhead) are seen with the fluorescence channel (a-c) and bright field overlay depicted (b-d). One of the deposits (asterisk) is cell-associated with a glial-like cell (a-b) whereas the other (arrowhead) is shown to be non-cell associated within the

neuroparenchyma (c-d). A green autofluorescence emission background was identified in non-stained sections, confirming the specific staining of Al deposits found (shown in Figure 3). Scale bar: 5 μ m.

Figure 5. Sheep 114, Adjuvant-only group, gray matter of the parietal lobe. (a-b) Lumogallion staining. Cell-associated, intense yellow-orange fluorescent Al deposits close to a blood vessel with the fluorescence channel (a) and bright field overlay depicted (b). (c-d) Sequential unstained sections for autofluorescence evaluation. A green autofluorescence emission background was identified in non-stained sections, confirming the specific staining of Al deposits found in (a) and (b), respectively. Scale bar: 10 μ m.

11. Synopsis of the Graphical Abstract

Subcutaneously inoculated aluminum hydroxide containing products triggers the formation of a postvaccination granuloma from where aluminum translocate to the regional lymph node and selectively accumulate in the gray matter of the lumbar spinal cord. Aluminum accumulation is higher with adjuvant only than with aluminum containing vaccines.

12. Highlights

- Aluminum-hydroxide is biodistributed from the subcutis to the central nervous system
- Aluminum is detected quantitatively and qualitatively in the lumbar spinal cord
- Aluminum is mainly found in the gray matter, mostly associated with glial-like cells
- Aluminum accumulation is higher after inoculation of adjuvant only than whole vaccines
- Results help to explain the ovine autoimmune/inflammatory syndrome induced by adjuvants

Control			Adjuvant-only			Vaccine		
Animal	Replicate N°	Al (µg/g)	Animal	Replicate N°	Al (µg/g)	Animal	Replicate N°	Al (µg/g)
131	1	0.19	111	1	1.24	121	1	0.93
	2	0.41		2	2.14		2	0.31
	3	0.05		3	14.36		3	0.39
132	1	0.03	112	1	0.29	122	1	0.36
	2	0.08		2	0.37		2	0.91
	3	0.38		3	0.56		3	0.82
133	1	0.01	113	1	7.83	123	1	0.58
	2	0.02		2	0.20		2	0.47
	3	0.46		3	7.83		3	0.32
134	1	0.58	114	1	0.49	124	1	0.47
	2	0.28		2	0.71		2	1.23
	3	0.01		3	0.35		3	0.33
135	1	0.52	115	1	0.84	125	1	0.35
	2	0.21		2	0.79		2	0.19
	3	0.00		3	0.24		3	0.45
136	1	0.01	116	1	0.29	126	1	0.39
	2	0.72		2	0.33		2	0.21
	3	0.01		3	0.15		3	0.35
137	1	0.01	117	1	0.48	127	1	0.65
	2	0.82		2	0.56		2	0.46
	3	0.06		3	0.48		3	0.32

Table 1. Aluminum (Al) content (µg/g) in the lumbar spinal cord of experimental sheep, measured by transversely heated graphite furnace atomic absorption spectroscopy (TH-GFAAS).

Control			Adjuvant-only			Vaccine		
Animal	Replicate N°	Al (µg/g)	Animal	Replicate N°	Al (µg/g)	Animal	Replicate N°	Al (µg/g)
131	1	0.01	111	1	0.13	121	1	0.79
	2	0.29		2	0.21		2	0.34
	3	0.36		3	0.88		3	0.40
132	1	0.17	112	1	0.32	122	1	0.84
	2	0.23		2	0.01		2	0.33
	3	0.16		3	0.08		3	0.01
133	1	0.01	113	1	0.20	123	1	0.71
	2	0.22		2	0.28		2	0.35
	3	0.48		3	1.01		3	0.23
134	1	0.01	114	1	0.02	124	1	0.01
	2	0.01		2	0.18		2	0.01
	3	0.35		3	0.08		3	0.08
135	1	0.01	115	1	0.74	125	1	0.08
	2	0.12		2	0.13		2	0.10
	3	0.39		3	0.72		3	0.33
136	1	0.01	116	1	1.29	126	1	0.01
	2	0.08		2	0.17		2	0.29
	3	0.01		3	0.14		3	0.01
137	1	0.09	117	1	0.37	127	1	0.01
	2	0.04		2	0.08		2	0.01
	3	0.01		3	1.36		3	0.10

Table 2. Aluminum (Al) content (µg/g) in the parietal lobe of experimental sheep, measured by transversely heated graphite furnace atomic absorption spectroscopy (TH-GFAAS).

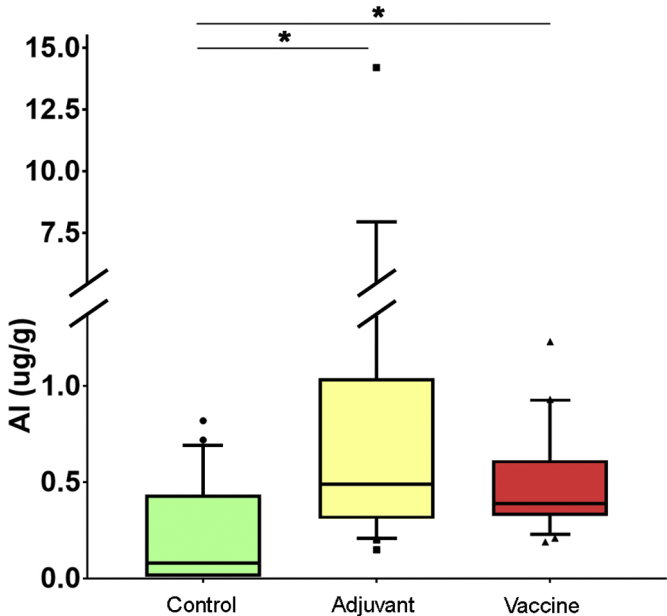


Figure 1

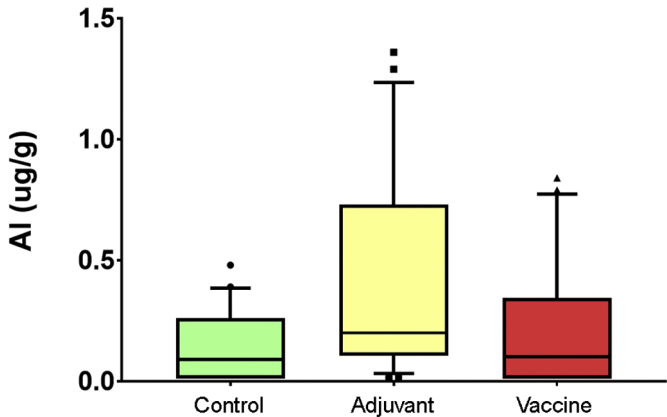


Figure 2

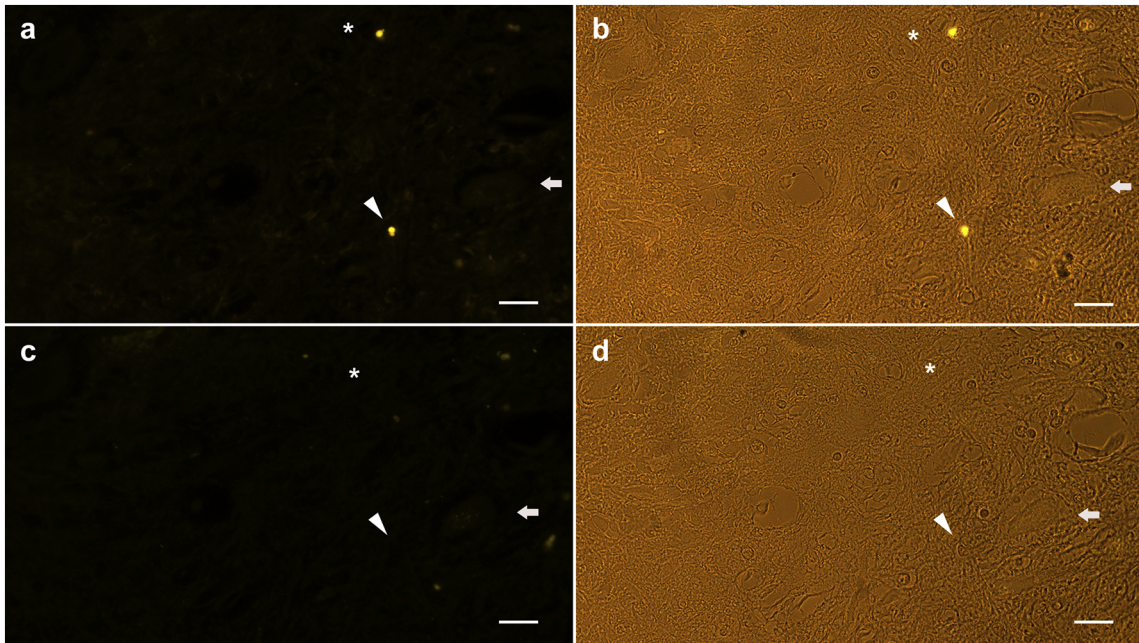


Figure 3

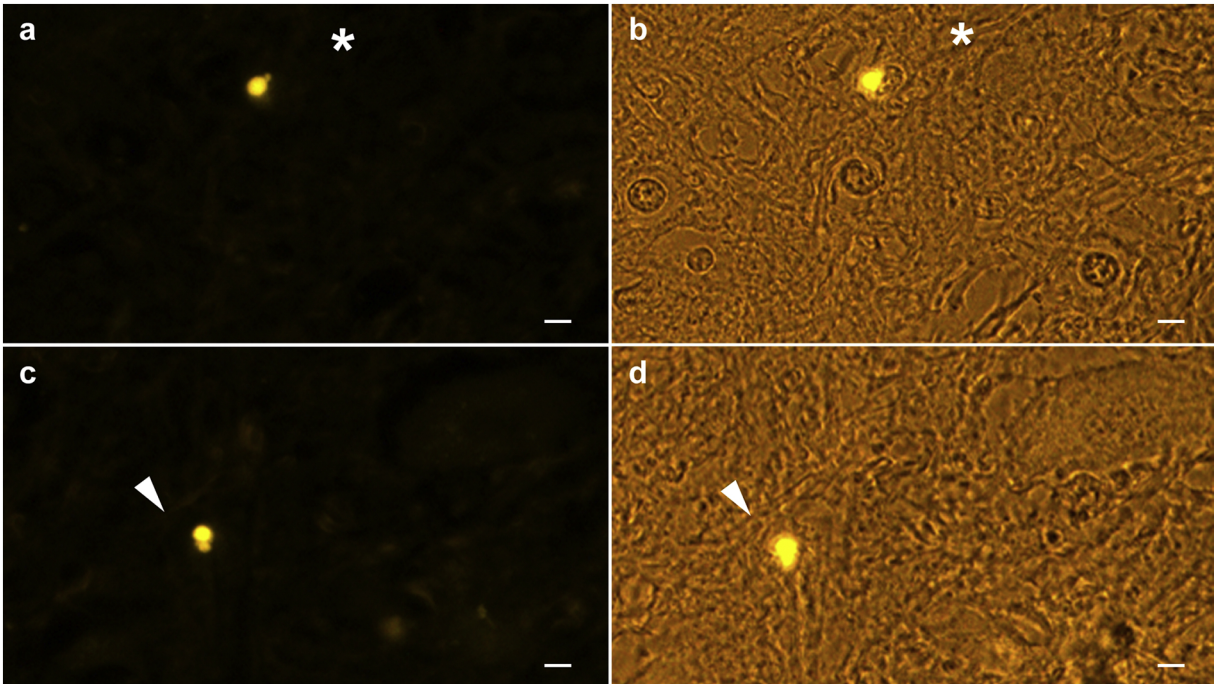


Figure 4

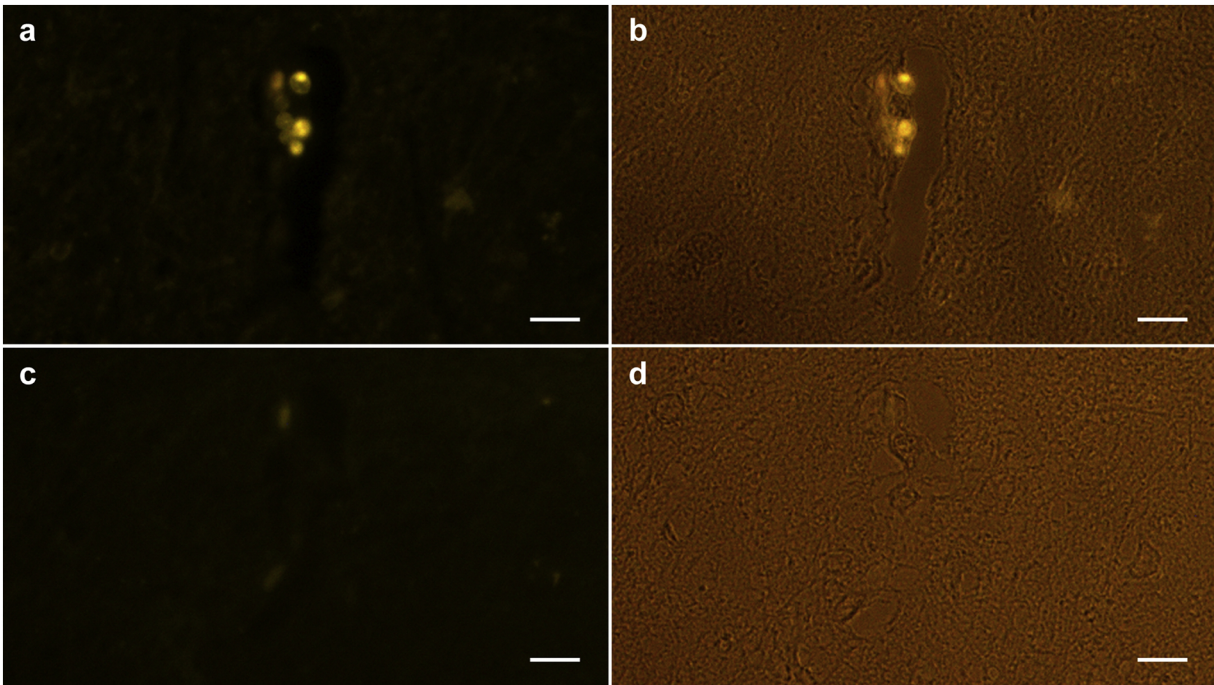


Figure 5